9

Magnet Coil and Flux Return

9.1 Physics Requirements and Performance Goals

The *BaBar* magnet is a thin, 1.5 T superconducting solenoid within a hexagonal flux return, as shown in Figure 9-1. Detector performance criteria and geometry considerations drive the design of the solenoid and the flux return. The magnitude and uniformity specifications for the magnetic field are derived from drift chamber track finding and momentum resolution requirements. Studies of $B^0 \to \pi^+\pi^-$ suggest that a magnetic field of 1.5 T is necessary to achieve a mass resolution of 21 MeV/c^2. The combined thickness of the vertex detector, drift chamber, particle identification system, electromagnetic calorimeter, and appropriate clearances set the solenoid inner diameter. Solenoid length is also determined by the length of the nested subsystems. The solenoid thickness limits the momentum threshold for detecting muons and the efficiency of K_L^0 detection within the instrumented flux return.

The segmented geometry of the flux return allows tracking of muons and provides for detection of K_L^0s with adequate angular resolution. The total thickness of the steel layers in the barrel and end door is determined both by the minimum steel required to avoid magnetic saturation and by the need for sufficient thickness to ensure that most of the pions interact in the steel. The minimal steel thickness to prevent pion punch-through is 55 cm ($\sim$3.6 λ_{int}). Plate segmentation and thicknesses are specified both for efficient identification of K_L^0 s and for distinguishing muons from pions based on range measurements. For more information on the meson detection system refer to Chapter 8.

The overall thickness of the flux return is the sum of both the steel thickness and the number and thickness of the RPC layers. Cost is also a factor in determining the number of RPC layers. Separation and movement of the end doors are constrained by beam line components and by the need to provide ready access to detector subsystems.

The physics performance and operational requirements for the solenoid and flux return (Table 9-1) are similar to those of many operating detector magnets (Table 9-2).

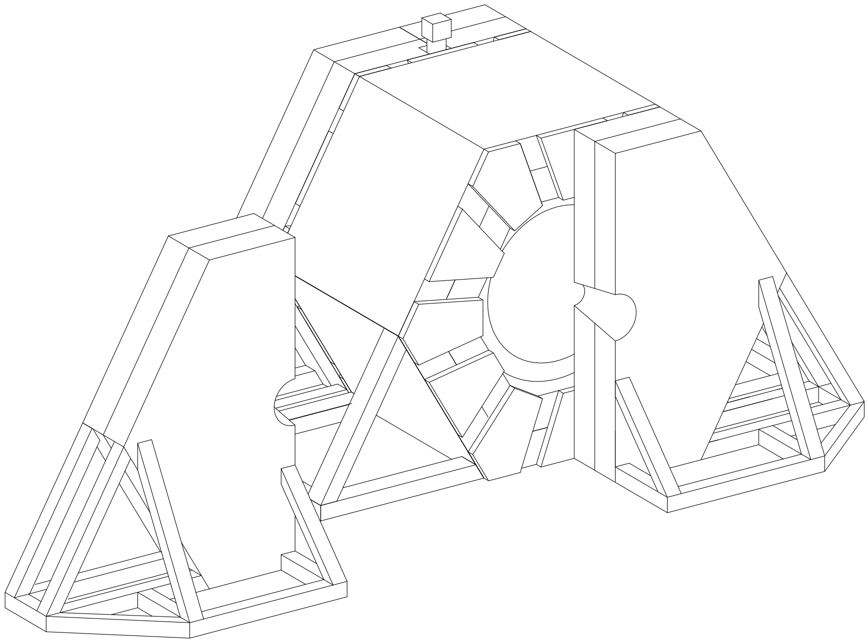

Figure 9-1. *Geometry of the solenoid within the flux return.*

9.2 Overview

The design of the superconducting solenoid for the *BaBar* detector is conservative and within the state of the art [Des85, And82, Coils] for detector magnets. It is based on the experience gained over the past 15 years with thin superconducting solenoids. Although specifically tailored to meet the requirements of *BaBar* (Table 9-1), this design is similar to many operating detector magnets. A common feature of all these magnets is the use of aluminum-stabilized conductors that are indirectly cooled by liquid helium pipes connected to an aluminum alloy support structure. This technique was developed for CELLO, the first thin solenoid, and has been improved in subsequent designs. Table 9-2 shows the main characteristics of some of these solenoids compared to the *BaBar* design. All of these designs used a Rutherford-type cable made of NbTi superconductor encased in an aluminum stabilizer that allows for adequate quench protection.

The *BaBar* detector schedule identifies the magnet as a critical procurement item. The three-and-one-half-year-long critical path is formed by: solenoid design and procurement; assembly with the flux return; verification testing and mapping; and detector subsystem installation and commissioning. While these task durations may be shortened, such reductions expose the project to higher budget and schedule risks. The solenoid design and fabrication duration

Solenoid Requirements	
Central induction	1.5 T
Field uniformity in the tracking region	$\pm 2\%$
Nuclear interaction length	0.25–0.4 λ_{int}
Cryostat inner radius	1400 mm
Cryostat outer radius	1730 mm
Minimize thermal cycling	$\surd$
Comply with ES&H requirements	$\surd$

Flux Return Requirements	
Provide an external flux path for a 1.5 T field	$\surd$
Provide 3 cm spacing between the steel plates for IFR instrumentation	$\surd$
Provide the gravitational and seismic load path for the barrel detector components to the concrete foundation	$\surd$
Fit in IR-2 (3.5 m radial distance from beam axis to the concrete floor)	$\surd$
Movable end doors to allow access inside the barrel	$\surd$
Comply with ES&H requirements	$\surd$

Table 9-1. *Physics performance and operational requirements.*

of 24–26 months requires the contract to be awarded in the fall of 1995 to meet the overall detector schedule.

The magnet cryostat will be designed, fabricated, and inspected according to the intent of the ASME Boiler and Pressure-Vessel Code, Section VIII, Division 2 [ASME94], but will not be code-stamped. The magnet will be subject to seismic design requirements described in the SLAC Seismic Design Manual for mechanical systems [SDM91]. The magnet design will also follow the requirements outlined in the Safety Analysis Document (SAD), which will address ES&H issues. For steel structures, the allowable design stresses follow the standard guidelines as specified in the AISC Manual of Steel Construction, 9th edition. Bolted connections and fasteners will conform to their recommended torques and allowable stresses depending on

	CDF	ZEUS	CLEO-II	ALEPH	BaBar
Location	FNAL	DESY	Cornell	CERN	SLAC
Manufacturer	Hitachi	Ansaldo	Oxford	Saclay	?
Year Completed	1984	1988	1987	1986	1997
Central Field (T)	1.5	1.8	1.5	1.5	1.5
Inner Bore (m)	2.86	1.85	2.88	4.96	2.80
Length (m)	5	2.5	3.48	7	3.46
Stored Energy (MJ)	30	12.5	25	137	25
Current (A)	5000	5000	3300	5000	7110
Total Weight (t)	11	2.5	7.0	60	6.5
Radiation Length	0.85	0.9	n/a	1.6	1.4 max
Conductor Dimensions (mm)	3.89×20	4.3×15, 5.56×15	5×16	3.6×35	3.2×30
Current Density (A/mm^2)	64	78	42	40	74

Table 9-2. *Comparison of solenoids similar to BaBar.*

the connection. The flux return is fabricated from ASTM A36 structural steel plates or a material with similar mechanical and magnetic properties.

9.2.1 Description of Key Interfaces

Superconducting Solenoid and Flux Return. The radial distance between the outer diameter of the solenoid and the inner surface of the barrel flux return is 50 mm. The solenoid weight and magnetic forces are transmitted to the inner and outer hexagonal rings of the flux return as shown in Figure 9-2. This attachment, located at the vertical mid-plane of the detector, also provides the load path of the inner detector components to the barrel flux return.

The backward end doors provide a chase for the cryostat chimney. The chase is 400 mm wide and extends 400 mm into the backward end doors.

Barrel and End Door. Both ends of the barrel flux return have a 60% solid steel contact area at the interface with the end doors. This area is composed of the 150 mm-thick inner ring support plates, 150 mm-thick joint braces, and 150 mm-thick steel gap filler plates. The remaining 40% open area on the barrel ends is reserved for cabling and utilities from the inner detector components. The end doors are attached to the barrel with tie plates that are bolted to the end door structure and to the barrel.

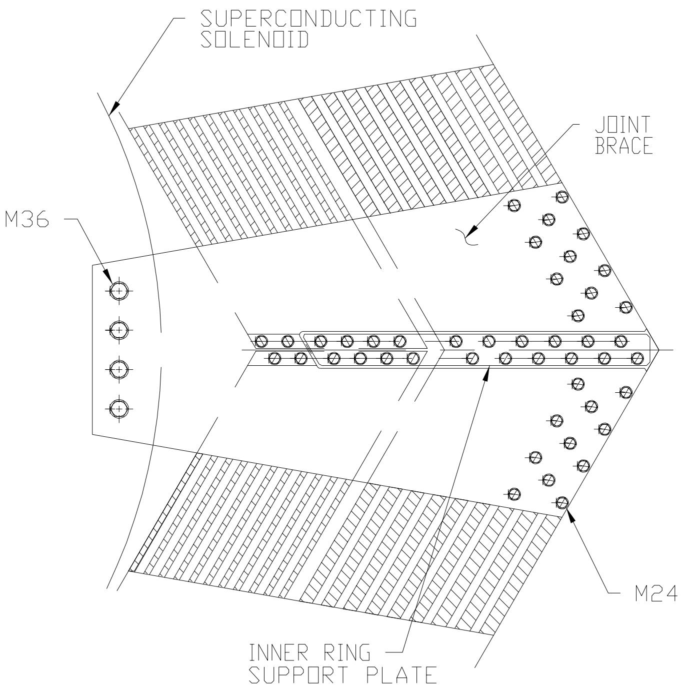

Figure 9-2. *Superconducting solenoid support bracket attached to the mid-plane of the flux return.*

Particle Identification System. A vertical slot between the backward end doors permits the support structure for the DIRC to penetrate into the detector. This structure also supports the backward beam magnets Q2, Q4, Q5, and the backward flux return field shaping plug located physically inside the DIRC. The final design details of the DIRC and the mounting of the backward beam magnets are not yet fully resolved.

Forward Q2 Beam Magnet Shielding. The forward beam magnet Q2 is physically located within the forward end doors. A specially designed, three-piece, conical magnetic shield plug is mounted to the end doors to isolate Q2 from the detector magnet. The shielding plugs are split along their vertical centerline, and each half is attached to a half-round mounting flange that is bolted to the face of each forward end door.

Inner RPC Detector and Solenoid. There is an RPC detector located between the calorimeter and the solenoid. This RPC detector attaches directly to the inner diameter of the solenoid cryostat with a 20 mm clearance gap between the RPC detector and the calorimeter.

Movable End Door Skids and the Beam Line. The end doors are mounted on skids equipped with rollers so that they can be moved away from the barrel for maintenance access. The end door skids move on tracks installed in the floor of IR-2. The end doors clear the beam line magnets, vacuum pumps, magnet stands, and other beam line equipment during door opening.

External Platforms, Stairways, and Walkways. The external platforms necessary to install and service electronic racks and cryogenic equipment are supported from the flux return. The requirements of these components have not yet been determined.

9.3 Summary of Projected Magnet Performance

9.3.1 Central Field Magnitude and Coil Performance

The magnetic field of 1.5 T is obtained by energizing the solenoid with a constant current of 7110 A. The conductor is operated at 45% of the critical current, with a peak field in the conductor of 2.5 T. This gives a large safety margin.

Magnetic uniformity is achieved by doubling the current density in regions at both ends of the solenoid. This is done by adding more aluminum stabilizer to the central region conductor, which reduces the current density there. Figure 9-3 shows the field uniformity in the central region. The areas in which the field nonuniformity is greater than 2% are small and are located in regions in which they do not affect the performance of the drift chamber. In addition, once the solenoid parameters are optimized, the corners of the drift chamber should also be within $\pm 2\%$ of 1.5 T.

The radial pressure on the conductor during operation is 1.5 MPa in the high current-density regions and 0.78 MPa in the central region of the conductor. An aluminum support cylinder surrounds the coiled conductor to react against these radial pressures and keep the conductor from yielding.

The integrated axial force on the winding is 3.5 MN. The conductor winding and support cylinder are mechanically coupled by an epoxy bond. This epoxy bond allows some of the axial load to be transmitted in shear to the outer aluminum cylinder, which keeps the conductor from yielding. There is an axial 18 kN de-centering force applied to the conductor winding due to an asymmetry in the iron, mainly due to the differences in the forward and backward Q2 shielding.

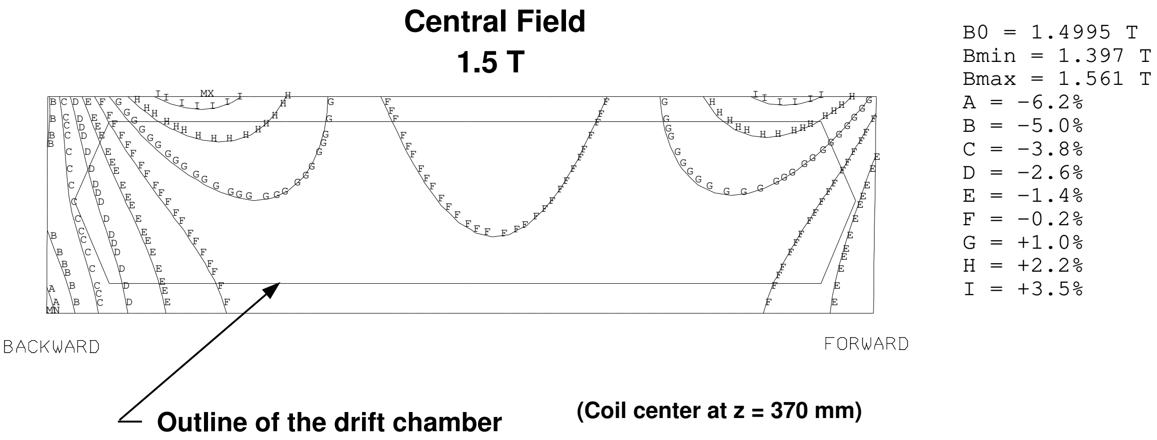

Figure 9-3. *Field uniformity inside the drift chamber. The central field is within ±2% of 1.5 T. Once the solenoid parameters are optimized, the corners of the drift chamber should also be within ±2% of 1.5 T. (The BABAR coordinate system is defined in Section 14.2.)*

9.3.2 Shielding of Forward Q2

The high luminosity of PEP-II requires that Q2, a non-superconducting septum quadrupole magnet, be placed close to the interaction region. Consequently, Q2 is situated within the forward end of the instrumented end door flux return (Figure 9-15). Q2 is subject to induced multipole moments resulting from the magnetic field in its vicinity, the octopole moment being the major one. The luminosity is critically dependent upon the Q2 field quality. Hence, it is necessary to provide adequate shielding of the *BABAR* central field to ensure the quality of the quadrupole field in Q2.

The present Q2 shield design is shown in Figure 9-4, where the three high-permeability shields (dark gray) surrounding Q2 (light gray) are visible, along with the logarithms of the magnetic equipotentials. The present design appears to shield Q2 from the detector magnet but does not provide a safety margin, should actual parameters, *e.g.,* steel permeability, differ from those used in the magnetic modeling programs. Work, including a full three-dimensional analysis, is continuing to improve the shield design.

9.3.3 Flux Return

The flux return assembly provides an external flux path for the magnetic field of the superconducting solenoid. Figure 9-5 shows the flux lines from the magnetic analysis. There are large body forces in the first few plates as a result of the magnetic field. Figure 9-6 shows

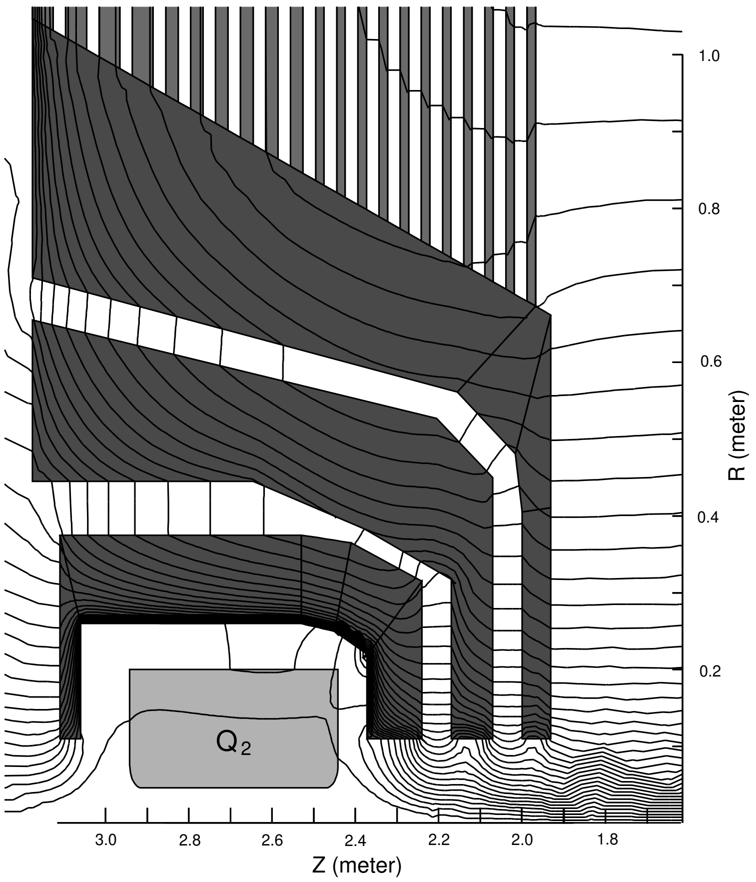

Figure 9-4. *Logarithms of magnetic equipotentials in the region of the Q2 septum quadrupole.*

the force vectors in the barrel and end doors of the flux return. Preliminary results show that stiffeners are needed in the end door plates to resist these axial forces. The present design has two stiffeners in each end door. As the end door design is refined, the locations and number of the plate stiffeners may change to keep the deflections and stresses in the plates within acceptable levels.

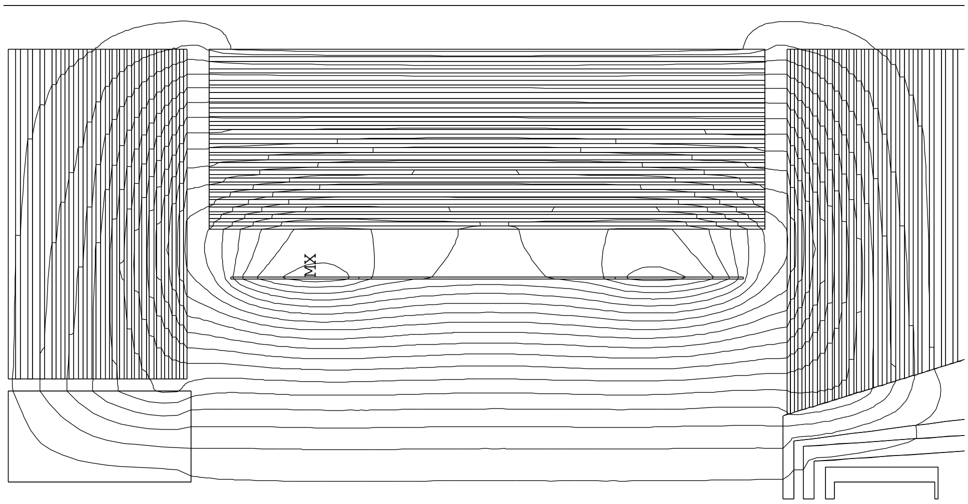

Figure 9-5. *Vector potential lines in the full detector region. The potential lines are horizontal in the region of the drift chamber, representing good field uniformity.*

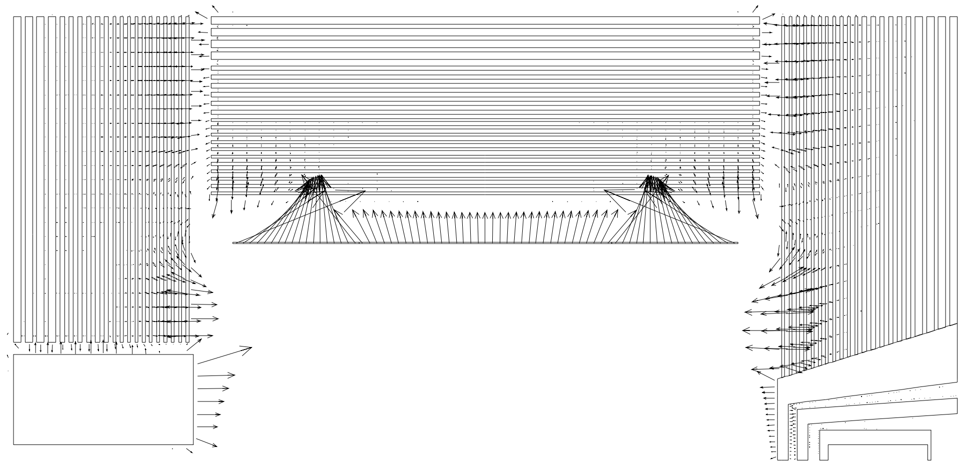

Figure 9-6. *Forces on the flux return plates, solenoid, and end plugs as a result of the magnetic field. The forces are the highest in the first few plates of the flux return.*

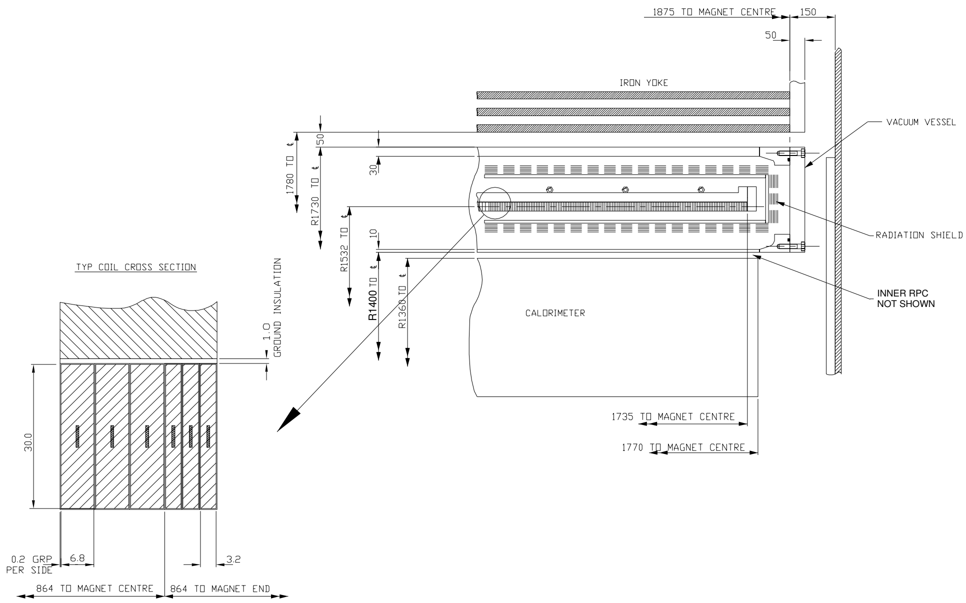

Figure 9-7. *Overall view of the solenoid showing the cryostat, both conductor cross sections, and radiation shielding.*

9.4 Superconducting Solenoid

9.4.1 Magnetic Design

This section describes the main features of the superconducting solenoid. For a more detailed description of the solenoid, refer to Reference [BF95]. A cross section of the solenoid is shown in Figure 9-7, and parameters are given in Table 9-3.

The magnetic analysis is based on a two-dimensional axially symmetric model. This model includes the solenoid, flux return plates, forward Q2 shield, backward shield, and the 150 mm gap between barrel and end doors.

The backward shield is designed to accommodate the DIRC. Its main functions are to improve the field uniformity in the backward region of the drift chamber and to balance the magnetic force on the solenoid due to the forward Q2 shield. A detailed design of this shield is underway. The iron properties used for computation (ANSYS code [ANS95]—two-dimensional magnetic element) are those of hot-rolled carbon steel.

The magnet design provides a magnetic field of 1.5 T with a uniformity of $\pm 2\%$ in the tracking region. This is obtained by grading the current density of the solenoid in three

Parameter	Value
Central Induction	1.5 T
Conductor Peak Field	2.5 T
Uniformity in the Tracking Region	$\pm 2\%$
Winding Length	3456 mm
Winding Mean Radius	1532 mm
Amp Turns	5.1192×10^6
Operating Current	7110 A
Inductance	0.985 H
Stored Energy	25 MJ
Total Length of Conductor	7000 m

Table 9-3. *Overall coil parameters.*

regions connected in series. The central region is 1728 mm in length with 240 turns. Two end regions are 864 mm in length with 240 turns each. The current density in the end regions is twice that of the central part. A better field uniformity may be obtained by reducing the axial length of the two end regions and increasing the current to generate the same field, but this would cause a reduction in stability against thermal disturbance. For the initial design, the maximum allowed current density in the conductor has been limited to the maximum currently attainable for magnets of this kind, *i.e.,* $\sim$80 A/mm^2 (ZEUS magnet). Thus, a cross section of $\sim$90 mm^2 for the smaller conductor corresponds to a maximum current of $\sim$7000 A.

Figure 9-5 shows the graph of the field lines over the full detector region. Figure 9-3 shows the field uniformity in the central region defined by $r < 800$ mm and $-1170 < z < 1910$ mm with respect to the IP. The magnetic field is essentially symmetric. A field uniformity of $\pm 2\%$ is obtained. Field uniformity is required up to $z = 1670$ mm in the forward region, and the present design provides a uniform field up to $z = 1910$ mm, providing a factor of safety. Further adjustment of the backward shield geometry may improve field symmetry, which would improve field uniformity in the backward region.

9.4.2 Cold Mass Design

Aluminum-Stabilized Conductor

The conductor is composed of a superconducting Rutherford cable embedded in a very pure aluminum matrix by a coextrusion process that ensures a good bond between aluminum and superconductor. Table 9-4 shows the main parameters of the conductor.

The operating current for this conductor is 45% of the critical current at the peak field, giving a large safety margin. In the case of local heating up to 5.2 K, there is still a significant margin on the critical current ($I = 0.6I_c$). At 2.5 T, the conductor-critical temperature is $T_c = 8.23$ K, and the current sharing temperature is 6.5 K. A simple method to evaluate the stability of the winding consists of considering the enthalpy margin per unit length between the operating and the sharing temperature. This stability parameter for the *BaBar* solenoid is 0.5 Joule/m, which is the same value obtained for the ALEPH magnet.

The cross section of the conductor is $3.2 \times 30\,\mathrm{mm}^2$ for the higher current density regions and $6.8 \times 30\,\mathrm{mm}^2$ for the central region. The coil winding can be made using six 1200 m lengths of conductor, requiring five electrical joints. Each joint, made by either welding of the aluminum matrix or soft soldering, has a resistance less than $5 \times 10^{-10}\,\Omega$ after the electro-deposition of copper, limiting the power dissipation to a few milliwatts.

Winding Support

The winding will be supported by an external aluminum alloy cylinder similar to other existing detector magnets. The winding support is designed for all aspects of force containment, *i.e.,* its weight and the radial and axial magnetic forces. Figure 9-6 shows these magnetic forces on the solenoid and the flux return.

The highest radial pressure, 1.5 MPa, is generated in the high current density regions at the ends of the coils. A pressure of 0.78 MPa is generated in the central region. An aluminum alloy (5083) support cylinder surrounds the coiled conductor to react against these radial pressures and prevent coil movement. The radial pressure is applied through the coil winding to the outer support cylinder. Assuming that the pure aluminum coil winding can be loaded to a stress of 20 MPa, the stress in the outer support cylinder can be estimated, using a thickness of 30 mm, to be 65 MPa. This stress of 65 MPa is well below the 170 MPa yield stress of the 5083 aluminum alloy. This simple analysis suggests that after the first charge the pure aluminum stabilizer will never be stressed beyond the elastic limit. This will help prevent premature quenching during coil energizing. A more complete analysis including both the Rutherford cable and the fiberglass epoxy insulation is not expected to significantly change the calculated stresses.

Parameter	Value
Conductor Type	NbTi, Pure Al-stabilized, Co-extruded
Aluminum RRR	> 500
Conductor Unit Length	1.2 km
Number of Lengths	6
Dimensions: Bare	3.2 and $6.8 \times 30.0\,\mathrm{mm}^2$
Insulated	3.6 and $7.2 \times 30.4\,\mathrm{mm}^2$
Superconducting Cable	Rutherford
Dimensions	$9 \times 1.23\,\mathrm{mm}^2$
Strands Diameter	0.84 mm
Number of Strands	20
Cu/Sc	1.8
Filament Diameter	$20\,\mu\mathrm{m}$
I_c ($B = 2.5\,\mathrm{T}$, $T = 4.5\,\mathrm{K}$)	$> 16\,\mathrm{kA}$
Insulation Type	Fiberglass Tape
Insulation Thickness	0.4 mm

Table 9-4. *Conductor parameters.*

An integrated compressive axial force of 3.5 MN is induced in the winding. The distribution of the axial force within the coil is complex. The end regions, with higher current density, compress the central part with 5.4 MN. The central part is axially stressed outward by a force of 1.9 MN. For preliminary calculations of the axial stress, the maximum force (6 MN) was considered. This would lead to an axial stress of 18 MPa on the pure aluminum, with only the winding supporting the axial forces. However, if the axial force is transmitted to the outer cylinder, the stress is lowered by a factor of two, with the pure aluminum working well below its elastic limit. In this case, the shear stress between the winding and outer supporting cylinder is less than 2 MPa. This low value of shear stress will allow the winding and support cylinder to be mechanically coupled through an epoxy impregnation without applying any axial prestress to the winding (as was done for the ZEUS magnet). Epoxy impregnation can support a shear stress higher than 20 MPa, providing a high safety margin. This leads to a simplification and cost saving in the winding fabrication.

The current design causes axial de-centering forces on the coil due to the iron asymmetry and a residual force of 18 kN is applied to the winding. A more careful design of the backward shield can help reduce the amount of this residual axial force by a factor of two or three.

Offset forces have been calculated as follows. An axial displacement of the solenoid of 10 mm causes an axial force of 98 kN in the direction of the displacement. A radial misalignment of 10 mm gives rise to a force of 89 kN. These values will be taken into consideration in designing the support system and should not present any significant problems.

Table 9-5 shows the main features of the cold mass. The values are given at a temperature of 4.5 K. The dimensions at room temperature are higher by a factor of approximately 1.004.

Electrical Insulation

Electrical insulation is an important aspect of solenoid design and manufacture. Two categories of insulation are required: ground plane insulation between the coil and support cylinder, and turn-to-turn insulation.

- The ground plane insulation must operate at relatively high voltages during quench conditions and will be subjected to strict QA controls. The design of the quench protection systems is based on a maximum voltage to ground of 250 V. The ground plane insulation will be made by a 1 mm layer of fiberglass epoxy laminate that is bonded to the support cylinder before winding. The insulation will be fully tested at 2 kV before winding.
- The conductor will be insulated with a double wrap of $\sim$0.1 mm glass tape during winding to give an insulation thickness of 0.2 mm. The resulting turn-to-turn insulation thickness will be 0.4 mm and will be fully impregnated in the bonding process. Electrical tests will be carried out during winding to detect any failure of insulation. The tests will include regular/continuous testing for turn-to-turn and turn-to-ground insulation.

9.4.3 Quench Protection and Stability

Protection Concept

The solenoid will be protected by an external dump resistor which will determine the current decay under quench conditions and allow extraction of $\sim$75% of the stored magnetic energy. The quench protection concept is shown in Figure 9-8, and quench parameters are given in Table 9-6. The protection concept is based on two main criteria.

- A voltage limit of 500 V across the solenoid applies during fast discharge. Center-tapping of the fast dump resistor to ground will limit the voltage to ground to 250 V. The center-tapped resistor will also allow the measurement of ground leakage currents as a safety and diagnostic tool.

Parameter	Value
Winding:	
ID	3033.8 mm
OD	3095.2 mm
Length	3456.0 mm
Weight	2.4 tonne
Supporting Cylinder:	
Material	Al alloy 5083
ID	3456.40 mm
OD	3516.40 mm
Length	3506.00 mm
Weight	2.5 tonne
Ground Insulation:	
Material	Fiberglass epoxy
Thickness	1.0 mm
Total Solenoid Weight:	4.9 tonne
Nuclear Interaction Length:	
(Assuming Aluminum)	
Maximum	0.19 λ_{int}
Minimum	0.15 λ_{int}

Table 9-5. *Cold mass (4.5 K) parameters.*

- An upper temperature limit of 100 K applies during quench conditions. This limit will give very good safety margins against peak temperature rise and thermally induced stresses at quench.

Quench Analysis

A preliminary quench analysis of the *BaBar* solenoid has been made using a code developed for the DELPHI solenoid design. The code models the thermal and inductive behavior of the solenoid in order to take into account quench-back effects and heat transfer to the support cylinder. This analysis shows that quench-back is predicted about two seconds after opening

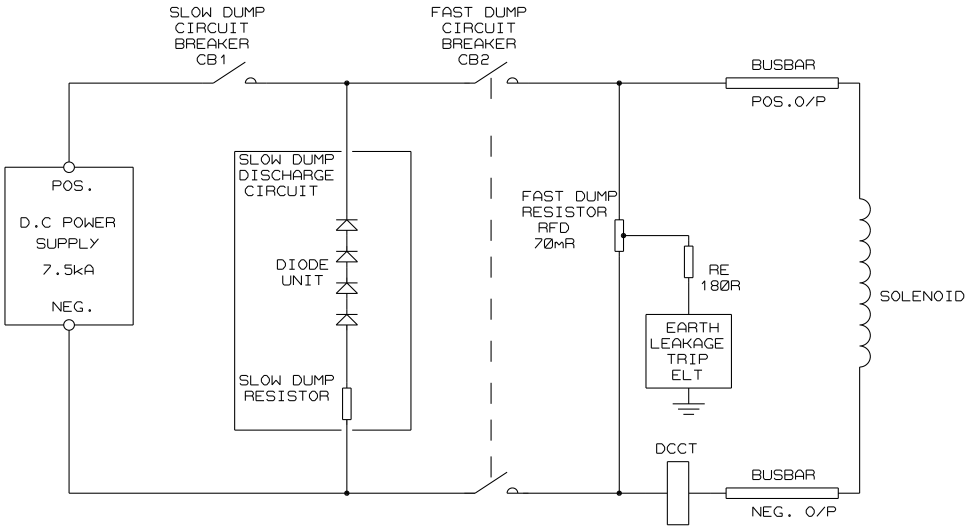

Figure 9-8. *Solenoid power and quench protection concept.*

Parameter		Value
Operating Current		7.11 kA
Stored Energy		25 MJ
Inductance		1.2 H
Quench Voltage		500 V
Protection Resistor		0.070 Ω
Time Constant		17.1 s
Adiabatic Peak Temperature		100 K
Overall Current Density:	Conductor 1	74 A/mm^2
	Conductor 2	35 A/mm^2
Aluminum Stabilizer RRR Zero Field		500

Table 9-6. *Quench parameters.*

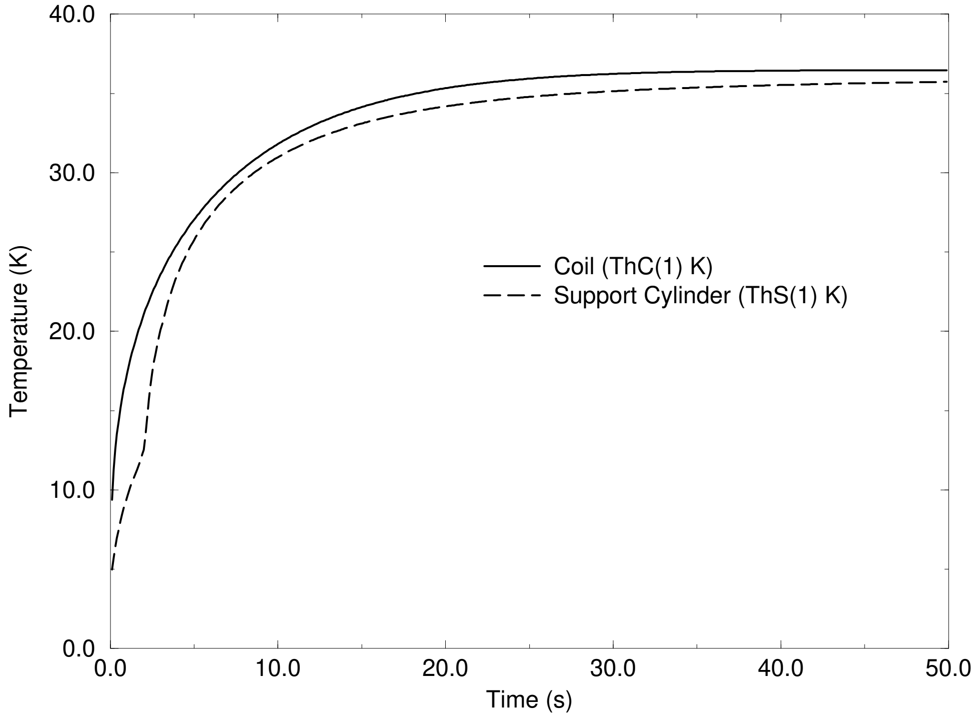

Figure 9-9. *Temperature variation during quench. The temperature rise in the coil and support cylinder during a quench should not exceed 40 K.*

the protection circuit breakers. Figure 9-9 shows that the temperature rise in the coil and support cylinder during a quench should not exceed 40 K.

Stability

The *BaBar* solenoid coil will be indirectly cooled using the technology established for existing detector magnets such as DELPHI and ALEPH. The reliable operation of those magnets has demonstrated that safe stability margins can be achieved using high-purity, aluminum-clad superconductors in a fully bonded, indirectly cooled coil structure.

Conductor stability has been estimated using an analysis code in order to establish the minimum quench energy (MQE) for transient heat pulses. The computed MQE = 1.4J. The computed minimum quench length (MQZ) is 0.6 m.

These margins are considered to be safe for the *BaBar* solenoid due to its low-stress design. The stability margin will be optimized during the full design study.

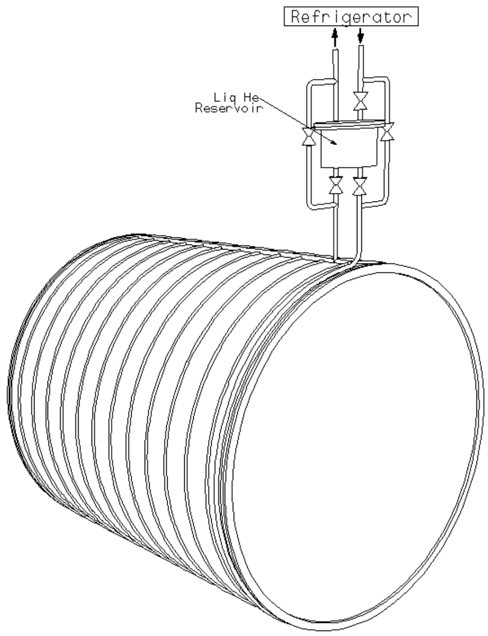

Figure 9-10. *Cold mass cooling circuit. The cryogenic supply chimney passes through a cut-out in the backward end of the barrel flux return.*

9.4.4 Cold Mass Cooling

Cooldown. Cold mass cooldown is accomplished by circulating cold helium gas either directly from the refrigerator or from a storage dewar with gas mixing. A preliminary cold mass cooldown analysis has been performed. A cooldown mass flow rate of $\sim$15 g/s will lead to a cooldown time of five days. The maximum temperature difference across the cold mass is limited to 40 K in order to minimize thermal stress during the cooldown from 300 to 100 K.

Operating Conditions. Under operating conditions, the cold mass is cooled by circulating two-phase helium in circuits mounted on the coil support cylinder. The thermo-syphon technique will be used to drive the cooling circuit. This technology is established and yields the simplest operational mode. The thermo-syphon cooling circuit is designed for high flow rates to ensure the correct quality factor for the helium. The conceptual layout of the cold mass cooling circuit is shown in Figure 9-10. The circuit is fed through a manifold at the bottom of the support cylinder. The cooling circuits are welded to the support cylinder surface with a spacing of $\sim$0.3 m to limit the temperature rise to less than 0.1 K. The cooling pipes terminate in an upper manifold. The circuit will be designed to provide operation during quench conditions.

Heat Loads. The estimated static heat loads for the solenoid are given in Table 9-7. Eddy current heating in the support cylinder will cause additional heat loads during charging of the solenoid. However, for a solenoid charging time of 30 minutes, the estimated transient power is $\sim$2 W, which is small compared to static heat loads.

9.4.5 Cryostat Design

Vacuum Vessel. The cryostat consists of an annular vacuum vessel equipped with radiation shields and superinsulation (Figure 9-7). The vacuum vessel is designed to satisfy a number of basic criteria:

1. Support vacuum loads in accordance with recognized pressure vessel codes;
2. Carry the cold mass and radiation shield weight through the insulating supports;
3. Operate with deflections of less than 2 mm under all loads when mounted in the flux return barrel;
4. Carry the loading of the inner detectors; and
5. Operate under defined seismic loadings.

The vacuum vessel is designed as two concentric cylinders with thick annular end plates, all of aluminum alloy 5083; its basic parameters are given in Table 9-8. A preliminary finite element (FE) structural analysis of the vessel has confirmed that design criteria (1)–(4) can be met with reasonable safety factors. Maximum vessel deflections are less than 2 mm, and stress levels are generally lower than 40 MPa with all loads applied. Deflections are minimized when the vessel is supported on the horizontal centerline and detector loads are also applied at that point. Performance of the vessel under seismic loadings (5) is still under consideration.

Thermal Shielding. The cryostat is equipped with radiation shields, which operate at 40–80 K, and superinsulation. The shields are cooled by helium gas supplied directly from the refrigerator. About 30 layers of superinsulation separate the vacuum vessel walls from the radiation shields. Another five layers will be installed between the shields.

Services. Cryogenic supplies and current supplies are connected from a services turret to the cryostat through the service chimney in the backward end door. Current leads and local control valves are mounted in the services turret. Cryogenic relief valves are also mounted in the service turret for quench and refrigeration failure conditions.

Magnet Heat Loads at 4.2K			
Item	Parameter	Load (watts)	Liquifaction (l/h)
Cold Mass	7000 kg		
Total Surface Area	100 m^2		
Radiation Heat Flux (Design)	0.4 W/m^2		
Radiation Heat Load (Design)		40 W	
Conduction Heat Load		10 W	
Transient Heat Load (30 min)		2 W	
Total 4.5 K		52 W	73 l/h

Magnet Shield Heat Loads at 80K			
Item	Parameter	Load (watts)	Liquifaction (l/h)
Shield Mass	1000 kg		
Total Surface Area	100 m^2		
Radiation Heat Flux (Design)	3 W/m^2		
Radiation Heat Load (Design)		300 W	
Conduction Heat Load		50 W	
Total 80 K		350 W	

Current Leads			
2 leads $\times$ 7 kA	0.72 g/s	16 W	22 l/h

Cryoplant Heat Loads at 4.2K			
Item	Parameter	Load (watts)	Liquifaction (l/h)
Valve Box and Valves		10 W	15 l/h
Transfer Lines (Liquefier-dewar & Return)	4 m ($\times$2)	6 W	8.5 l/h
Transfer Line (Dewar-valve Box)	4 m	3 W	4 l/h
Coaxial Transfer Line (Valve Box-magnet)	60 m	3 W	4 l/h
4000L Dewar		6 W	8.5 l/h
Total 4.2K		28 W	40 l/h

Table 9-7. *Cryogenic heat loads.*

Envelope Dimensions	
Inner Radius	1400 mm
Outer Radius	1730 mm
Length	3850 mm
Materials	AL5083
Design Loads	
Vessel Weight	6 tonne
Cold Mass	6 tonne
Calorimeter	50 tonne
Seismic Load Factors (Max)	
Horizontal	1.2 g
Vertical	2.0 g

Table 9-8. *Vacuum vessel parameters.*

9.4.6 Coil Assembly and Transportation

The coil will be assembled inside the cryostat at the manufacturer's plant. Electrical and cryogen connections will be made at the chimney so that the coil can be tested before shipping.

A complete cooldown will be carried out from room temperature to the operating temperature of 4.5 K. The cooldown will allow checking of cooldown time, temperature control, heat loads, and full operation of sensors. A magnetic test will also be performed at low field (30% of the operating current) to check superconductor operation, the joint resistance, and the additional losses due to the energization.

Before delivering the magnet, but after the tests at the factory, the end flanges will be dismounted to allow a hard connection of the cold mass to the cryostat walls. Depending on the transport facilities, the chimney may also be dismounted. In this case, the electrical and cryogen connections also must be dismounted and protected against breakage.

9.5 Cryogenic Supply System and Instrumentation

Operation of the superconducting solenoid requires both liquid helium and cold helium gas (20 K to 100 K) for cooldown and refrigeration of the thermal shields. Similar systems have been used successfully throughout the HEP community. A summary of the cryogenic loads is given in Table 9-7.

The helium plant, consisting of a helium liquefier/refrigerator, a 4000 ℓ supply dewar, and a distribution valve box (DVB), is located adjacent to the experimental hall, approximately 60 m from the magnet, as shown in Figure 9-11. It is possible that the DVB will be incorporated within the helium liquefier cold box, depending upon the helium liquefier selected. This liquid helium plant meets all of SLAC's requirements and is sized conservatively at 150–200 ℓ/hr. It will supply LHe to the *BaBar* superconducting solenoid, the two future superconducting beam line focusing magnets (Q1), and an auxiliary dewar/trailer for all other SLAC experiments. The detector solenoid is expected to consume less than 100 ℓ/hr of LHe.

Liquid nitrogen is required for the helium liquefier, for the initial stages of coil cooldown, and miscellaneous uses in IR-2. It will be supplied from a 20,000 ℓ tank located on the apron above the experimental hall. This tank, which is an existing SLAC unit, will be refurbished to serve all cryogenic system requirements. A second, similar vessel is also available if a reserve LN2 supply is required. Vacuum-insulated transfer lines connect the LN2 tank to the helium plant.

The 4000 ℓ liquid helium dewar is a refurbished SLAC unit fed directly from the liquefier. This volume provides approximately 30 hours of autonomous operation of the solenoid and quadrupole magnet systems in the event of a minor liquefier/compressor malfunction. LHe from the dewar is supplied at $\sim$1.25 bar, via proportional control valves in the DVB, to the appropriate magnet/auxiliary dewar system as required. These electro-pneumatic operated valves are actuated by process controllers and superconducting LHe level gauges.

Liquid helium and cold helium gas are supplied to the detector solenoid and Q1 superconducting magnets in flexible, vacuum-insulated, low-loss transfer lines. These transfer lines provide the cold gas return path to the liquefier/refrigerator. This type of transfer line has been used successfully by SLD. The transfer lines are designed to be compatible with the SLD lines so that the latter can serve as spares and/or Q1 transfer lines. LHe and cold shield gas for the solenoid are routed to the magnet service chimney at the detector backward end door penetration (north end). Magnet cooldown to $\sim$20 K is achieved with cold helium gas via the DVB. Warm helium gas from magnet current leads is routed in uninsulated piping to compressor suction.

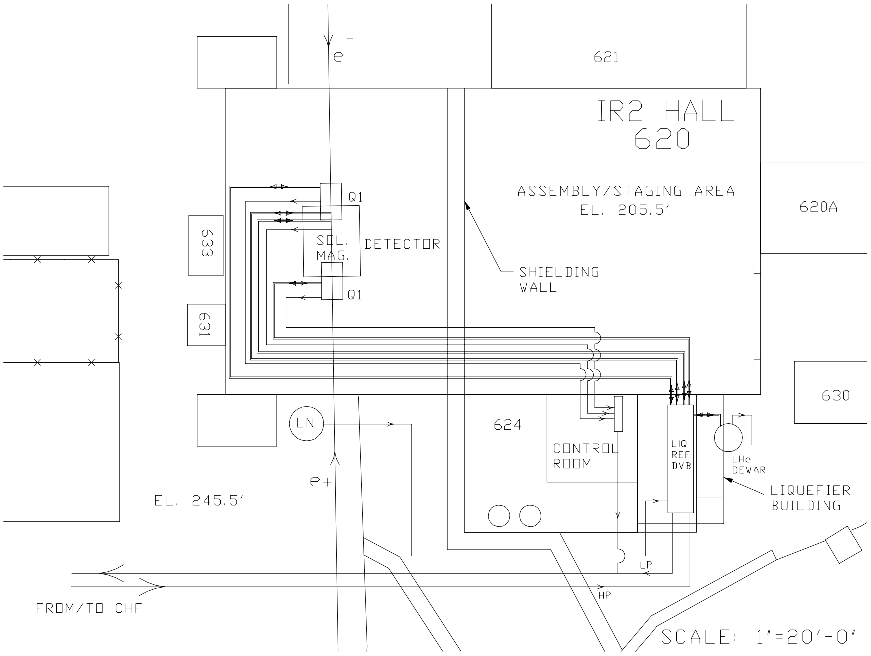

Figure 9-11. *Layout of the cryogenic system.*

The solenoid is equipped with a full set of instrumentation sensors for monitoring, control, and diagnostic purposes. Instrumentation includes temperature sensors for the cold mass, shield cryogen flow monitoring, and strain gauges in the coil support cylinder. Voltage taps monitor the electrical resistance of the conductor joints and quench detection. The quench detection systems are hard-wired to interlocks. The solenoid instrumentation and controls are integrated with the *BaBar* experiment and refrigeration controls.

The liquid helium plant, which is fully automatic, is furnished with a process control system and all requisite logic and software necessary for all operational modes. Control and monitoring of the cryogenic plant and the magnet coil, together with remote control and monitoring of the compressor room, is carried out from a control room adjacent to the plant room and IR-2. Main operating parameters are interfaced with the *BaBar* data acquisition and monitoring systems.

9.6 Flux Return

9.6.1 Overview

The flux return assembly provides the external flux path for the magnetic field from the superconducting solenoid. The steel plate segmentation enhances low momentum pion/muon separation and K_L^0 detection efficiency. The flux return also provides the gravitational and seismic load path for the barrel detector components to the concrete foundation.

The flux return assembly consists of a barrel, four external support legs, two sets of end doors, roller mechanisms, and vertical adjustment systems. The design of the flux return and its components reflects the limitations of the IR-2 experimental hall.

End door components must be movable once the detector is assembled to allow maintenance access to inner detector subsystems. The design of the flux return provides a means for proper alignment of all flux return components with respect to the detector magnet and the beam line. This alignment must be reestablished after maintenance is performed.

Analysis of the Flux Return

The flux return analysis will investigate the overall structural integrity, including that of the supporting structures. This includes looking at all the components and connections involved in the operation, assembly, and seismic loadings of the structure. Operating loads for the barrel include both the gravitational and the magnetic forces. Assembly loads include any additional fixture weights that need to be attached during assembly. Seismic loadings assume a site-specific peak ground acceleration of 0.6 g. This seismic design standard exceeds that of the minimum base shear requirements as formulated by the Uniform Building Code.

A finite element model program, ANSYS [ANS95], revision 5.1, is currently being used to study the stresses and deflections of the barrel and its supporting structures under the different loading conditions. It is also being used to model the structure's response to oscillatory ground motion. The results from these studies will be used to verify that the design requirements are met.

9.6.2 Barrel Flux Return Description

The barrel flux return assembly is shown in Figure 9-12. The barrel flux return assembly extends 4050 mm in z, and the center is positioned 370 mm from the interaction point in

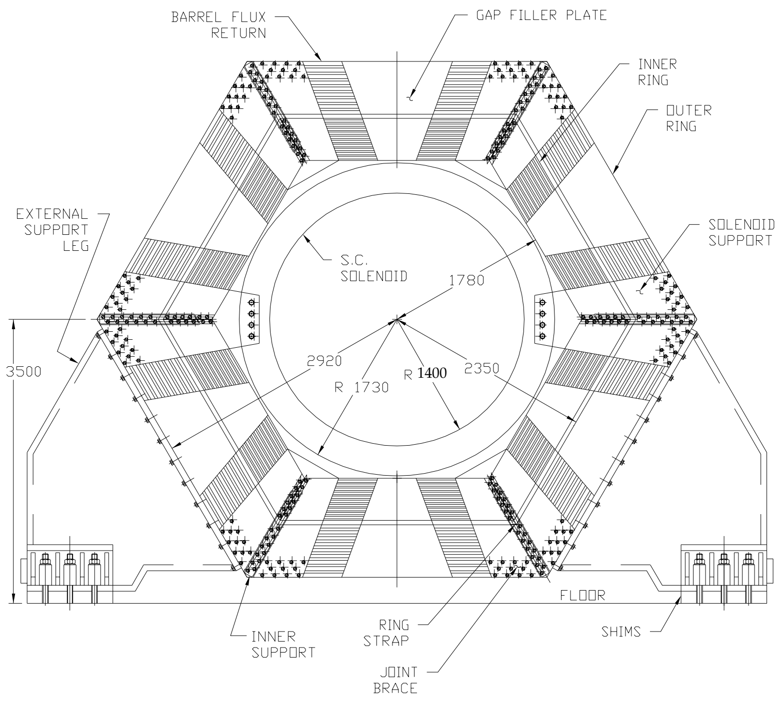

Figure 9-12. *Barrel flux return assembly showing the support of the solenoid, gap filler plates, and the external support legs.*

the positive z direction. The barrel flux return extends radially from the detector axis from 1780 mm to 2920 mm and consists of inner and outer hexagonally-shaped concentric steel rings. The radial gap between the inner and outer rings is 50 mm. The rings consist of blocks with multiple steel plates oriented parallel to the axis of the solenoid. Two side plates and the inner and outer parallel plates of each block are welded into a rigid box using full penetration welds along their entire length in the z direction (parallel to the beam line). The remaining parallel plates are held in place using skip welds at their connections with the side plates. The use of double block construction for each of the hexagonal segments of the barrel flux return provides a significant safety margin with respect to the 45-tonne rated capacity of the overhead crane in IR-2. The blocks are designed to provide continuous muon detection in azimuth. The weight of the barrel flux return is 312 tonne excluding the external support legs.

Outer Ring Description

The outer ring is the primary structural support for the *BaBar* detector. This ring is composed of six blocks. Each block consists of six 30 mm-thick and three 50 mm-thick parallel

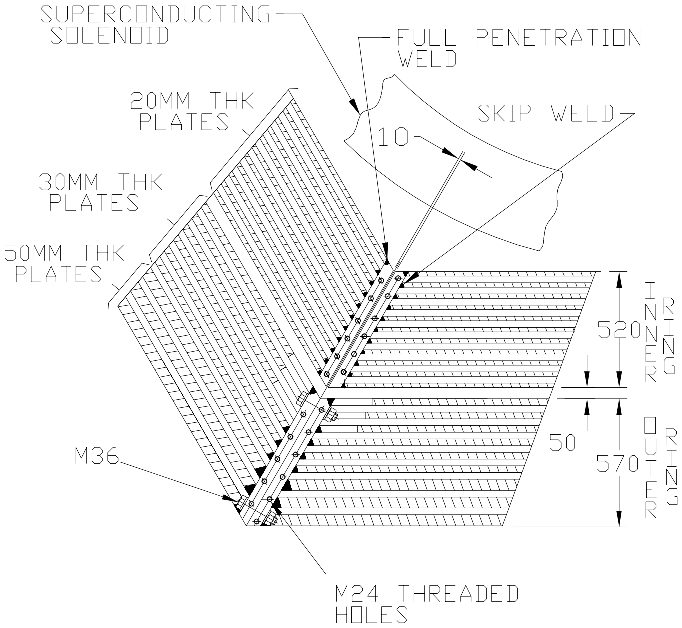

Figure 9-13. *Block-to-block interface in the flux return.*

structural plates oriented so that the thicker plates are positioned towards the outermost portion of the barrel hexagon. The plates are positioned in each block to provide 30 mm of clear space between each plate and the next for the installation of Resistive Plate Chambers (RPCs). The inner surface of the outer block is located 2350 mm radially from the interaction point. The 30 mm spacing between plates is to be maintained during block fabrication. Therefore, the tolerance build-up due to variations in the plate thickness and plate flatness extends outward in the radial direction. The spacing of the parallel plates is held fixed by 60 mm-thick side plates located at the block-to-block interface, as shown in Figure 9-13. Two of the blocks are provided with threaded holes in their outer plates for mounting of the external support legs. Each block is 3750 mm in length, 570 mm in nominal height, 2714 mm wide at the inner trapezoid base, and 3372 mm wide at the nominal outer trapezoid surface. Each outer block weighs approximately 31.2 tonne.

Inner Ring Description

The inner ring is also composed of six blocks. Each block consists of eleven 20 mm-thick parallel structural plates positioned to provide 30 mm of clear space between plates for the installation of RPCs. The inner surface of the inner block is located 1780 mm radially from the interaction point. Like the outer plates, the 30 mm spacing is held fixed, and the plate manufacturing tolerances are allowed to accumulate in the outward direction. A gap

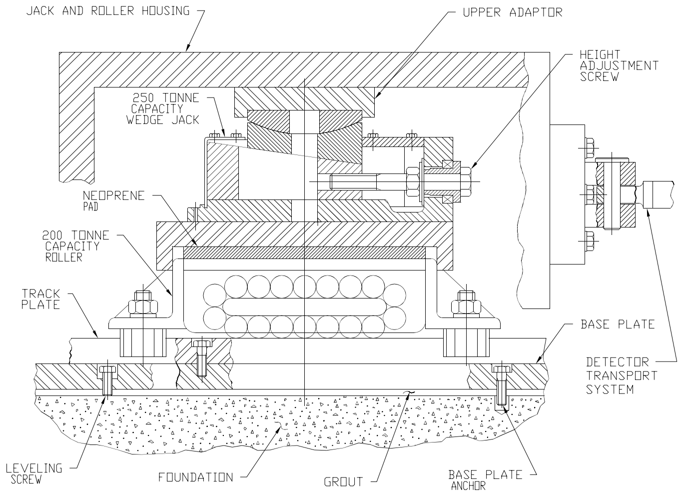

Figure 9-14. *A 200 tonne capacity roller and a 250 tonne capacity jack are located at the end of each support leg to support the barrel.*

of 20 mm is provided between the inner and outer hexagonal rings for this purpose. The spacing of the parallel plates is held fixed by 50 mm-thick side plates located at the block-to-block interface as shown in Figure 9-13. The side plates are provided with threaded holes to mount a 150 mm-thick plate that supports the inner blocks from the outer ring. The inner blocks are 5 mm shorter in z length than the outer blocks and will have to be shimmed during assembly for a secure fit. There is 10 mm of clearance provided at the block-to-block connections for manufacturing and assembly tolerances. Each block is 3745 mm in length, 520 mm in nominal height, 2050 mm wide at the inner trapezoid base, and 2650 mm wide at the nominal outer trapezoid surface. Each block weighs approximately 16.4 tonne.

External Support Legs

Two external support leg assemblies provide the gravitational and seismic load path from the barrel flux return to the concrete foundation. Each assembly consists of two legs positioned 3200 mm apart in z. The legs are fabricated from 50 mm-thick structural steel plates. Included at each support leg is a 200 tonne capacity roller and a 250 tonne capacity jack as illustrated in Figure 9-14. A preformed fabric pad is positioned between the jack and the roller to add compliance to the system. The horizontal spacing of the jack and roller assemblies is nominally 8000 mm. Each support leg is approximately 3750 mm in length, 2400 mm in width, and 3300 mm in height. The weight of each support leg assembly is approximately 20 tonne.

9.6.3 End Door Description

The forward and backward end doors are an array of steel plates that form a regular hexagon approximately 5840 mm across the flats and 1120 mm thick. The array consists of eleven 20 mm-thick plates, six 30 mm-thick plates, and three 50 mm-thick plates. There is a nominal gap width of 30 mm between plates in the array for locating the RPCs. The plates for both the forward and backward end doors weigh approximately 255 tonne. This weight does not include plates and bars that tie the plates together for structural reasons, the support members that attach the end doors to a movable skid, or the skid itself (Figures 8-23 and 9-15). Both the forward and backward end doors are split along the vertical centerline of the detector forming right and left end doors.

Each end door is mounted on a skid that permits it to be raised onto high load capacity rollers by hydraulic jacks and to be moved on tracks located in the IR-2 hall. This provides a means to move the end doors into proper alignment with the barrel prior to being bolted in place, and to be moved away from the barrel for maintenance access to the detector. The center of gravity of the end door plates is high compared to the depth of the base. The skid provides additional stability during the horizontal accelerations experienced during moving or seismic events.

During operation, the magnet exerts an inward axial force that causes a significant bending moment on the end door plates. The forward end doors also support the weight of the Q2 shielding plug and carry the axial magnetic load induced in the plug. To resist gravitational and seismic loads, and to limit the plate stresses and deflections, all the end door plates are joined together to form a single structural member.

The design of the end doors permits each door to be assembled and disassembled inside the IR-2 hall with the existing facility crane. Since the capacity of the IR-2 crane is 45 tonne, each separable part, together with all rigging and lifting fixtures needed, cannot exceed this limit. Each end door is therefore composed of two weldments that are fastened together at installation. The inner weldment consists of eleven 20 mm plates and two 30 mm plates, with each plate welded to a channel-shaped frame that extends along the top and bottom of the hexagon shape and along the boundary between the right and left doors. Two horizontal stiffeners are positioned between the 20 mm plates. Additional stiffeners are also required to stiffen the weldment and help maintain the necessary gaps for the RPCs. The outer weldment consists of four 30 mm plates and three 50 mm plates welded together with similar stiffening members. The detailed analysis of the response of the plates to the magnetic force distribution is not yet available, nor has a detailed seismic analysis been done for the end door plates. Several design options are being studied that can provide the necessary strength and stiffness.

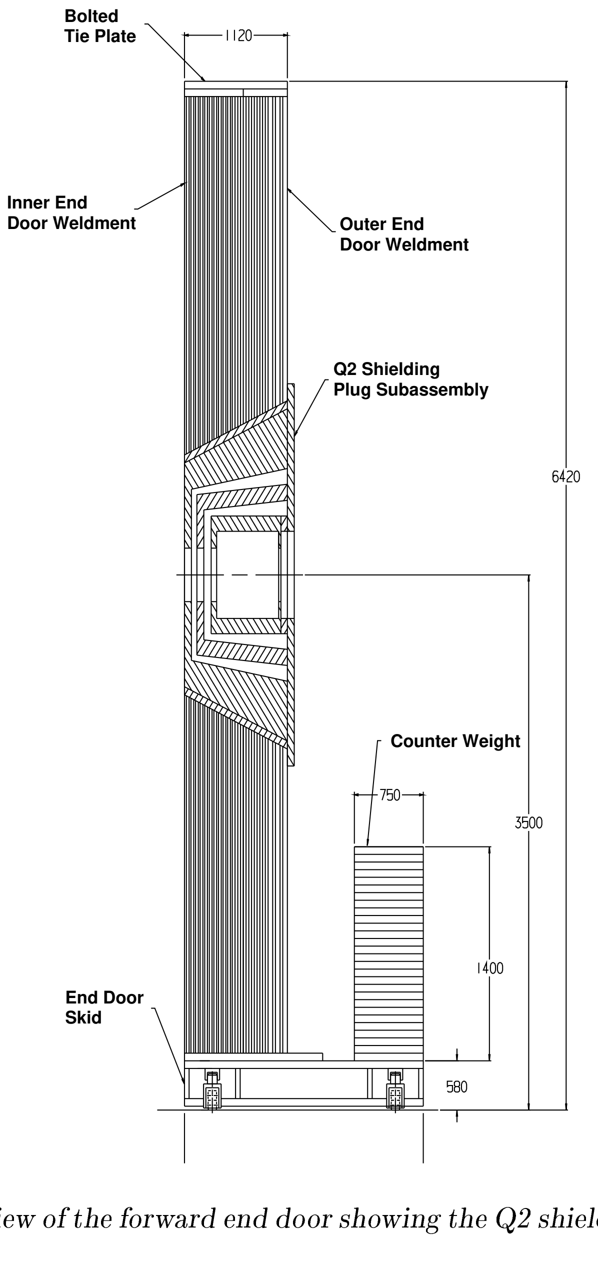

Figure 9-15. *Side view of the forward end door showing the Q2 shielding, counter weights, and support rollers.*

The inner and outer weldments are joined together at installation by bolting each weldment to the top of the skid along the bottom of the hex, and by bolting tie plates around the remaining perimeter of the weldments, except where the shielding plugs are located. The outside tie plates are bolted in place after the RPCs are installed, and provisions for cabling are provided in these outside plates. These tie plates are also used to attach the end doors to the barrel of the flux return.

End Door Skids

Each end door is mounted on a skid that is equipped with four 70 tonne capacity rollers, and four 45 tonne hydraulic jacks, one in each corner, which allow each of the doors to be moved relative to the barrel for maintenance access. The rollers ride on hardened steel tracks that are permanently located in the floor of IR-2. Because the bases of the end doors are narrow compared to their high centers of gravity, 30 tonne of existing scrap steel is bolted to each skid to lower the center of gravity and move it toward the middle of the skid.

The end doors are bolted either to the barrel of the flux return when in the operating position or to seismic restraint brackets when in the parked position. While the doors are being moved, the 30 tonne counter weight provides lateral stability for a horizontal acceleration of 0.3 g.

Forward Q2 Shielding Plug Support

The preferred option for mounting the Q2 shielding plug is to fabricate and assemble the shield in two sections split along the vertical axis. These assemblies are mounted to large half-round flanges that are bolted to the back 50 mm plates of the forward end doors (Figure 9-15). This simplifies access to the front portion of the detector when the end doors are moved. It is likely that the halves of the end door will be tied together by two additional half-round flanges oriented at 90° to the shielding plug supports to stiffen the assembly. This option requires that each half of the shield be installed in the end doors at final assembly since each half of the shield assembly weighs approximately 20 tonne. Special lifting and assembly fixtures are required to accomplish this task.

The alignment of the shield and the Q2 magnet is done by adjusting the position of each half-round flange on the end door and installing dowel pins to maintain the alignment. Sufficient clearance between the shield and the forward Q2 magnet is provided to permit the shield to move vertically with the stroke of the jack as the end door is raised to be rolled out of the way for detector access.

9.6.4 Options and Detailed Design Issues

A detailed stress and deflection analysis is proceeding for the finalized overall envelope dimensions. A detailed magnetic field and force analysis of the end doors ensures that they will have adequate strength and stiffness to meet all the requirements imposed on them.

The tolerance on plate flatness must be defined together with the envelope dimensions of the RPCs. Standard mill tolerances for plate flatness do not meet our requirements for the end door plates to permit reliable RPC installation; these tolerances exceed 15 mm, half the nominal gap width. This issue, together with weld distortion in the plates during fabrication, must be resolved with both the plate supplier and the barrel and end door fabricator. Other manufacturing tolerances must be established as the system interface dimensions are finalized, and the effects of these tolerances on the physics performance of the detector are reviewed.

9.6.5 Procurement, Fabrication, Assembly, and Schedule

The barrel and the end doors will be built by the same fabricator as part of the same procurement contract. This will eliminate some duplication in the review of vendor qualifications, quality control plans and actions, and many contract administration issues. In addition, control of other characteristics of the plate material, such as the chemistry of the plates as it affects weldability and machinability, the mechanical properties of the plate, *etc.*, may be more easily tracked by having one set of acceptance inspection criteria from one supplier for all plates.

The barrel and end doors will be fully assembled and inspected at the fabricator's shop. In this way, any problems that arise can be solved before final assembly in the IR-2 hall. This will also permit a thorough review of the assembly procedure by an experienced fabricator and ensure that the necessary lifting and assembly fixtures are functional and are provided with the barrel and end doors. The details of the fabrication and assembly plan will be developed by the fabricator subject to the review of the responsible design engineer in the *BaBar* collaboration.

References

[And82] D. Andrews *et al.,* "A Superconducting Solenoid for Colliding Beam Experiments," Ad. Cryogenic Eng. **27** (1982).

[ANS95] ANSYS, INC, "General Finite Element Code," Rev. 5.1 (1995).

[ASME94] ASME, "1992 ASME Boiler and Pressure Vessel Code" (1992).

[BF95] E. Baynham and P. Fabbricatore, "Superconducting Solenoid for the BaBar Detector," *BaBar Note* in preparation.

[Coils] A. Bonito Oliva *et al.,* "ZEUS Magnets Construction Status Report," 11th Int. Conference on Magnet Technology, MT–11, 229 (1989).
P. Clee *et al.,* "Towards the Realization of Two 1.2 T Superconducting Solenoids for Particle Physics Experiments," 11th Int. Conference on Magnet Technology MT–11, 206 (1989).
H. Desportes *et al.,* "Construction and Test of the CELLO Thin-Wall Solenoid," Ad. Cryogenics Eng. **25**, 175 (1980).
H. Desportes *et al.,* "General Design and Conductor Study for the ALEPH Superconducting Solenoid," J. Phys. (Paris) **C1-341**, S1-T45 (1984).
Y. Doi *et al.,* "A 3T Superconducting Magnet for the AMY Detector," *Nucl. Instr. Methods* **A274**, 95 (1989).
M.A. Green *et al.,* "Construction and Testing of the Two-Meter-Diameter TPC Thin Superconducting Solenoid," Ad. Cryogenics Eng. **25**, 194 (1980).
M.A. Green *et al.,* "A Large Superconducting Thin Solenoid for the STAR Experiment at RHIC," IEEE Trans. App. Superconductivity, 104 (1993).
H. Hirabayashi, "Detector Magnet Technology for High Energy Accelerators," ICEC–11, 115 (1986).
H. Minemura *et al.,* "Fabrication of a 3 m-dia. $\times 5$ m Superconducting Solenoid for the Fermilab Collider Detector Facility," J. Phys. (Paris) **C1-333**, S1-T45, (1984).
C.M. Monroe *et al.,* "The CLEO-II Magnet–Design, Manufacture, and Tests," ICEC–12, 773 (1988).
M. Wake *et al.,* "Excitation of a Superconducting Large Thin Solenoid Magnet," MAG–23, 1236 (1987).
F. Wittgenstein *et al.,* "Construction of the L3 Magnet," 11th International Conference on Magnet Technology, MT–11, 131, (1989).
A. Yamamoto *et al.,* "Thin Superconducting Solenoid Wound with the Internal Winding Method for Colliding Beam Experiments," J. Phys. (Paris) **C1-337**, S1-T45 (1984).

[Des85] H. Desportes, “Recent Progress in the Design and Construction of Beam and Detector Magnets,” in Proceedings of the Int. Symposium on Magnet Technology (Zurich, Switzerland), MT–9, 149 (1985).

[SDM91] Earthquake Safety Committee, “Seismic Design Manual - Mechanical,” Rev. 1 Stanford Linear Accelerator Center, Stanford, California (1991).